

SCIENTIFIC REPORTS



OPEN

Single-step generation of metal-plasma polymer multicore@shell nanoparticles from the gas phase

Pavel Solař¹, Oleksandr Polonskyi², Ansgar Olbricht², Alexander Hinz², Artem Shelemin¹, Ondřej Kylián¹, Andrei Choukourov¹, Franz Faupel² & Hynek Biederman¹

Nanoparticles composed of multiple silver cores and a plasma polymer shell (multicore@shell) were prepared in a single step with a gas aggregation cluster source operating with Ar/hexamethyldisiloxane mixtures and optionally oxygen. The size distribution of the metal inclusions as well as the chemical composition and the thickness of the shells were found to be controlled by the composition of the working gas mixture. Shell matrices ranging from organosilicon plasma polymer to nearly stoichiometric SiO₂ were obtained. The method allows facile fabrication of multicore@shell nanoparticles with tailored functional properties, as demonstrated here with the optical response.

Production of metal nanoparticles (NP) by gas aggregation sources (GAS) that utilize magnetron sputtering and buffer-gas condensation has become a fast-growing field in nanoscience^{1–5}. Sputtering can supply atomic metal vapors from solid targets into a gas phase in a controllable manner. By adjusting the parameters of the discharge, the partial pressure of metal vapors can be deliberately increased above the target surface to create the conditions of supersaturation. Such far-from-equilibrium conditions can be further enhanced by using a cool buffer gas which may trigger spontaneous condensation of metal vapors and the formation of NPs. Typically, a buffer gas flow is created in the aggregation zone to transport NPs away from the magnetron and deposit them onto solid supports.

Originating in the 1990s, work on the use of magnetron-based GASes for the production of single-metal NPs^{6–9} was followed by research on multi-metal NPs. The combination of two (or more) metals at the nanoscale was found to provide NPs with unique properties and extra functionality. The state-of-the-art involves using a single magnetron with a composite target or multiple magnetrons in a single GAS. It was recognized that multi-metal NPs of different morphology can be produced, for example, nanoalloy^{10–13}, core@shell^{2, 14–18} or Janus NPs^{19, 20}.

Fabrication of composite NPs composed of materials other than metals can significantly broaden the functionality of NPs. Possible applications include protection of metal NPs from oxidation, fine tuning NP plasmonic response and functionalization of NPs for controlled drug delivery and biosensing. Composite NPs with metal core and dielectric shell were successfully produced using wet chemical methods^{21–23} or combinations of physical and chemical methods²⁴. These, however, usually need multiple production steps and typically suffer from the use of toxic precursors, the elimination of the residuals of which represents a substantial challenge. From this viewpoint, gas phase methods of fabrication of composite NPs may prove advantageous albeit they have been studied much less²⁵.

In this paper, we present a method for the production of metal core@plasma polymer shell NPs that combines buffer-gas induced condensation of magnetron-sputtered silver and plasma-enhanced chemical vapor deposition (PECVD) of hexamethyldisiloxane (HMDSO). The aim of the research is to investigate the feasibility of such an approach and to find tools to tune the morphology and chemical composition of NPs by setting the appropriate experimental conditions.

Experimental

Nanoparticles (NPs) were produced using a gas aggregation cluster source (GAS) with a 2-inch magnetron equipped with either a graphite or a silver target (both 6 mm thick, 99.99% pure, Kurt J. Lesker). The magnetron was placed inside a cylindrical aggregation chamber capped with a conical lid with a circular orifice 3 mm in diameter and 0.5 mm in length. The GAS chamber was cooled by water at 20 °C. The magnetron was powered by

¹Charles University, Faculty of Mathematics and Physics, Department of Macromolecular Physics, Prague, 182 00, Czech Republic. ²Kiel University, Faculty of Engineering, Chair for Multicomponent Materials, 24143, Kiel, Germany. Correspondence and requests for materials should be addressed to P.S. (email: pawell.solar@seznam.cz)

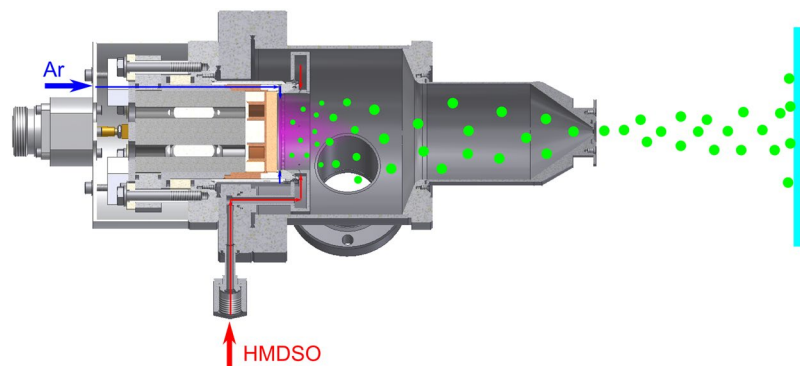


Figure 1. Schematics of the gas aggregation cluster source and the gas inlet system.

an RF generator (Dressler Cesar, 13.56 MHz) through a matching box. Constant power of 50 W was chosen for the experiments. Argon (99.9999%) was supplied through a flow controller (MKS Instruments) between the powered electrode and the magnetron shielding directly to the target, as shown in Fig. 1. Hexamethyldisiloxane (HMDSO, 98.5% pure, Sigma Aldrich) was supplied to the GAS from a flask via a needle valve. The HMDSO inlet ends in a gas ring positioned 15 mm away from the surface of the target. The gas ring had several holes, all directed towards the target. The experiments were performed at 190 Pa pressure in the GAS with the flow rate of Ar fixed at 105 sccm. The concentration of HMDSO was varied by changing its flow rate from 0.02 to 0.45 sccm. In a number of the experiments, O₂ (99.9999%) was added to the Ar/HMDSO mixture.

The GAS was mounted onto a high vacuum deposition chamber pumped by scroll and turbo-molecular pumps to a base pressure below 10⁻⁴ Pa. The NPs were deposited on different substrates (quartz glass, TEM grids, gold coated silicon substrates) positioned in the deposition chamber 20 cm from the exit orifice of the GAS. The samples were analyzed by transmission electron microscopy (TEM, JEM-2100, JEOL, 200 kV, LaB6), UV-Vis spectroscopy (Ellipsometer Woollam M2000 UI), X-ray photoelectron spectroscopy (XPS, Omicron Nanotechnology GmbH) and Fourier Transform Infrared Spectroscopy (FTIR, Bruker Equinox 55). In the case of XPS measurements, all spectra were charge referenced for aliphatic carbon at 285.0 eV.

Results and Discussion

Plasma polymerization of organic precursors often leads to the formation of nano- and micro-scale particles in the gas phase. Organic molecules supplied to the plasma zone undergo fragmentation followed by gas-phase radical recombination and form nuclei, the process being especially effective if performed under an elevated pressure of tens to hundreds of Pa²⁶. Chemical composition of the resultant particles is given by the type of precursor used and by the energetic conditions of the plasma. Particle structure can typically be represented by a highly cross-linked and random carbonaceous network²⁷. Figure 2a shows an example of the NPs prepared by the GAS with a mixture of Ar and HMDSO and a graphite target attached to the magnetron. The NPs were produced with a mean size of 36 nm and with the XPS elemental composition of C 52%, Si 30%, O 18%, very similar to the HMDSO films and NPs reported earlier^{28,29}. The TEM image in Fig. 2b shows the result of the same experiment performed when the graphite target was replaced by a silver one. In this case, heterogeneous NPs are produced and consist of distinct multiple cores enveloped by a shell of the plasma polymer. XPS analysis shows the appearance of silver, although the concentration of other elements remains almost the same (Ag 2%, C 52%, Si 25%, O 21%). Remarkably, the mean size of the multicore@shell NPs does not change when compared to the NPs without the multicores. The diffraction pattern characteristic for silver was detected by TEM and is shown in the right column of Fig. 2.

Magnetron sputtering of metals is known to result in the supply of an atomic metal vapor into the gas phase. The metal vapor may spontaneously condense with the formation of NPs if the conditions of supersaturation are fulfilled, and recent years have witnessed the successful application of GASes for the production of beams of metal NPs^{8,30,31}. Here, the magnetron sputtering of silver is evidently accompanied by plasma polymerization processes of HMDSO-derived radicals and the formation of Ag NPs is accompanied by competitive growth of HMDSO plasma polymer. It is known that cohesive forces between noble metal atoms greatly exceed the interaction energy between metals and organics, polymers in particular. As a consequence, metals do not form one phase with polymers but both tend to segregate into two phases³². Within the framework of low-temperature plasma deposition, the phase segregation leads to the generation of metal/plasma polymer nanocomposites, either in the common form of thin films^{33–36} or in the form of core@shell NPs presented here. It is also worth noting that the growth does not lead to the formation of individual core@shell NPs, as might be and was originally expected, but the groups of several Ag NPs become embedded in a single plasma polymer shell. It seems reasonable to assume that individual core@shell NPs are formed in the vicinity of the magnetron target and later coalesce with each other on their way through the aggregation chamber, thus generating the multicore@shell structure. A similar phenomenon was recently observed for ternary magnetron synthesis of inorganic NPs composed of multiple FeAg cores encapsulated by a Si shell^{37,38}.

Addition of oxygen to HMDSO is known to trigger oxidation processes in the plasma. Reactive oxygen species consume carbon with the formation of volatile oxides that do not participate in plasma polymerization. This in turn leads to the production of carbon-deficient deposits that are consequently more inorganic. The process

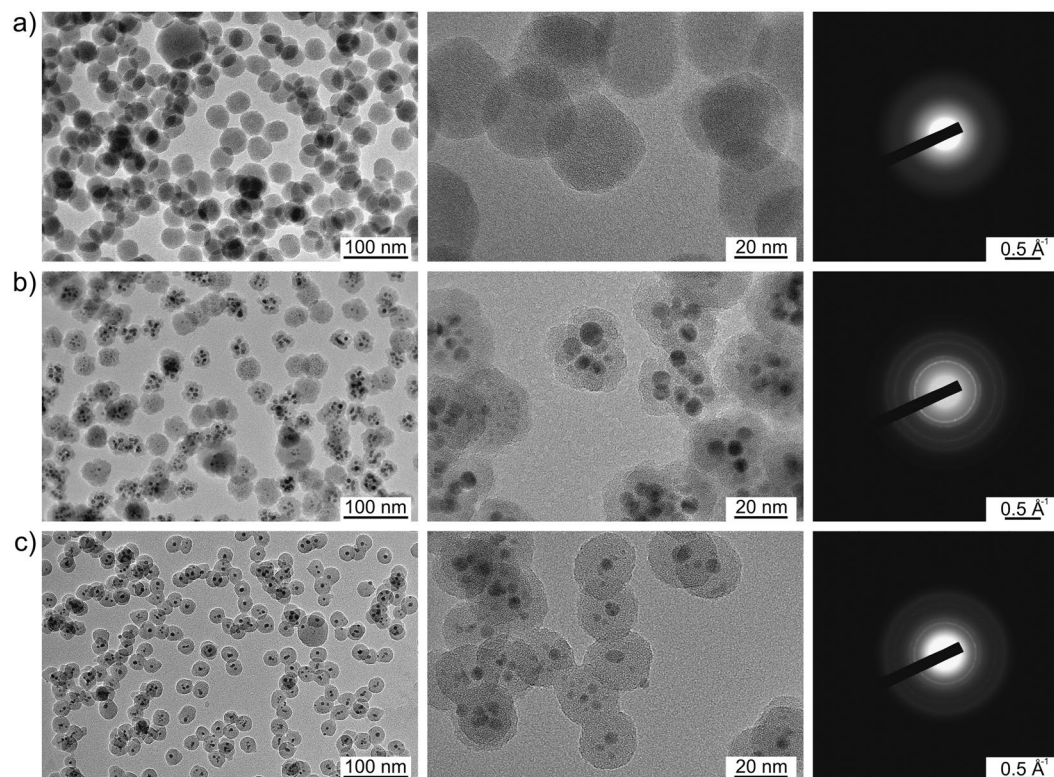


Figure 2. TEM images with lower (left column) and higher (middle column) magnification of the NPs prepared by GAS: (a) from the Ar/HMDSO mixture with graphite target and (b) from the Ar/HMDSO mixture with Ag target (in both cases the HMDSO flow rate is 0.45 sccm); (c) from the Ar/HMDSO/O₂ mixture with Ag target (0.15% HMDSO, 3.8% O₂, Ar flow rate 105 sccm, pressure 190 Pa). The right column shows the corresponding diffraction patterns.

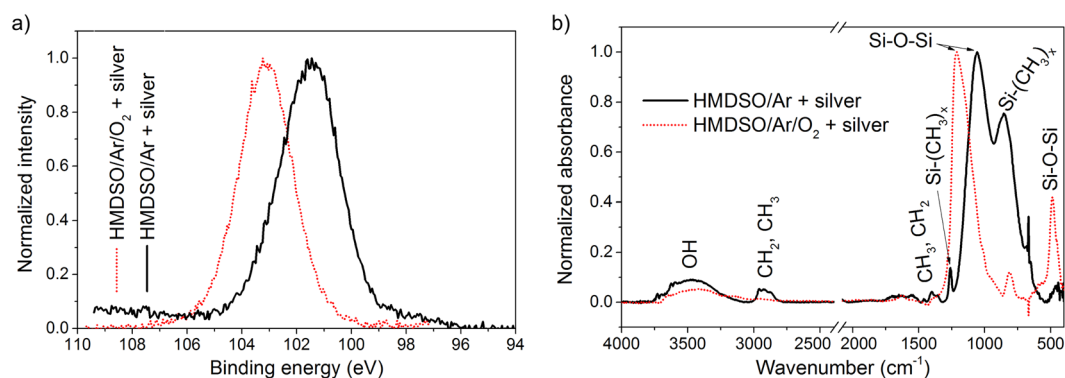


Figure 3. Chemical analysis of the NPs prepared by GAS from the Ar/HMDSO mixture with or without the addition of O₂: (a) high-resolution Si 2p XPS; (b) FTIR-RAS.

can be optimized to produce stoichiometric SiO₂ in the form of thin films or nanoparticles²⁹. Figure 2c shows the result of such optimization performed in the GAS with the silver target. The addition of 4% of O₂ to the Ar/HMDSO mixture leads to the fabrication of NPs with embedded multiple Ag inclusions with 5 nm average size. The XPS composition shows Ag 4%, C 3%, Si 32%, O 61%, which indicates that the shell consists of nearly stoichiometric SiO₂. No diffraction pattern characteristic of crystalline silicon dioxide was detected, which points to an amorphous state of the shell. The formation of SiO₂ is also corroborated by high-resolution XPS, which shows a higher binding energy shift in the position of the Si 2p peak from 101.6 eV for the Ar/HMDSO mixture without O₂ to 103.1 eV for the mixture with O₂ (Fig. 3a). Furthermore, the FTIR-RAS spectra of both types of NPs also reveal the chemical changes from the organic to the predominantly inorganic SiO₂ character (Fig. 3b). The addition of O₂ leads to the disappearance of the bands associated with vibrations of the hydrocarbon and organosilicon groups (see, for example, CH_x stretching at 2960–2870 cm⁻¹ and Si-(CH₃)_x rocking at 850 cm⁻¹).

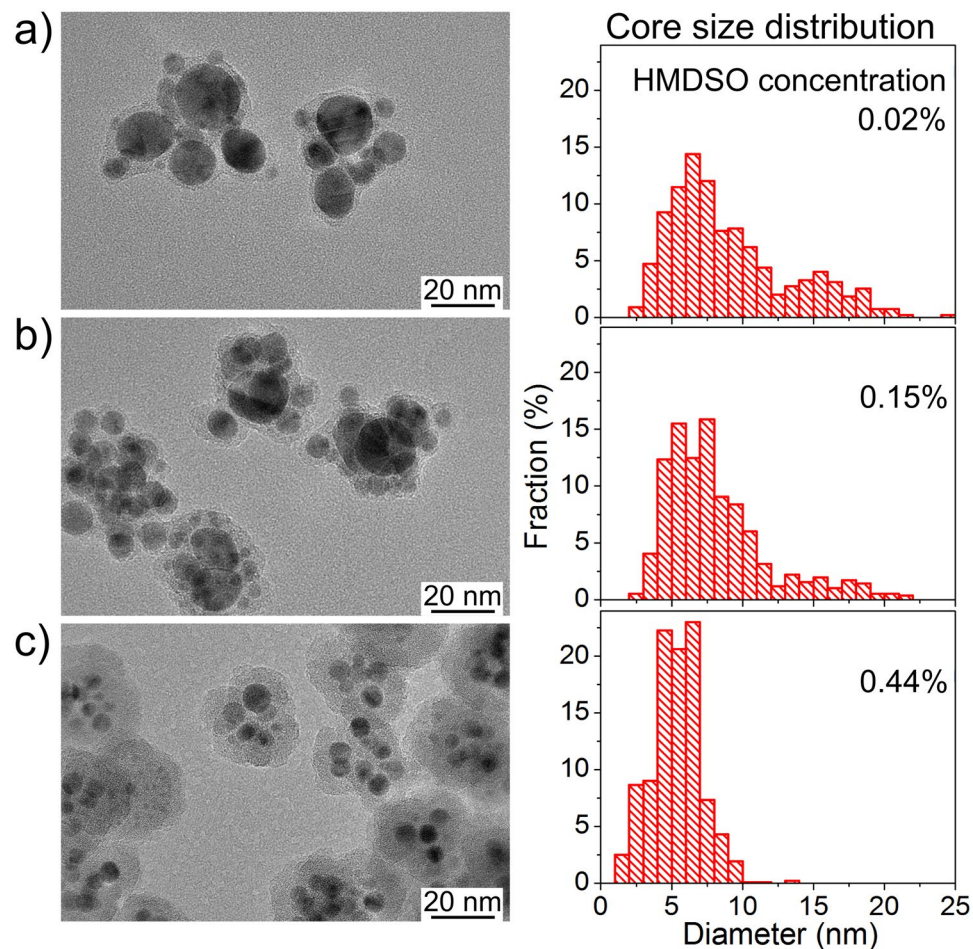


Figure 4. TEM images and the core size distributions of the multicore-shell NPs prepared by GAS at different concentrations of HMDSO: (a) 0.02%, (b) 0.15%, (c) 0.44%.

Simultaneously, a siloxane rocking band develops at 485 cm^{-1} , whereas the corresponding stretching vibration shifts from 1050 to 1210 cm^{-1} , which also reflects the disappearance of an organic bonding environment^{33,39}.

Another set of experiments was performed without the addition of O_2 but with different concentrations of HMDSO in Ar. All other parameters were held constant. The size of the Ag inclusions was found to decrease and the thickness of the plasma polymer envelope to increase, with the HMDSO concentration increasing from 0.02% to 0.44% (Fig. 4). The phenomenon is accompanied by the narrowing of the Ag NP size distribution, as can be seen from the corresponding histograms. The XPS analysis supports these findings by showing the decrease of the silver content from 27 at. % to 2 at. % with the increasing thickness of the plasma polymer shell (increasing concentration of HMDSO).

The UV-Vis measurements of the multicore@shell NPs provide spectra with a strong absorption band from localized surface plasmon resonance (LSPR) (Fig. 5). At the lowest HMDSO concentration, the band occupies a region between 400 and 600 nm, a large width of which is caused by the large dispersity in Ag NP size. Also, note the presence of two shoulders in this band that likely originate from the bimodal size distribution of the Ag NPs detected in the sample (Fig. 4). In further agreement with the TEM observations, the increase of HMDSO concentration leads to a narrowing of the LSPR absorption band, and corresponds to a narrower Ag NP size distribution. The position of the band at 445 nm is red-shifted with respect to <400 nm typically obtained for similarly sized bare Ag NPs³¹. The red-shift of the LSPR band has been well documented in the literature, the shift being larger for embedding dielectric media with greater refractive index⁴⁰. Here, the shift is readily attributed to the influence of the HMDSO plasma polymer matrix separating the Ag NPs as compared to bare Ag NPs separated by air voids. It also confirms that the Ag NPs are completely embedded within the plasma polymer shell.

Conclusion

An effective single-step method for the gas-phase production of metal@plasma polymer nanoparticles was developed and is based on the use of a gas aggregation cluster source for simultaneous rf magnetron sputtering of a metal target and PECVD of an organic precursor. Silver NPs were successfully embedded in an organosilicon plasma polymer shell. Advantageously, the method also involves the formation of multicore@shell instead of a single-core@shell morphology of NPs. The concentration of HMDSO is found to be an important parameter influencing the size distribution of the Ag inclusions as well as the optical activity of the resultant multicore@shell

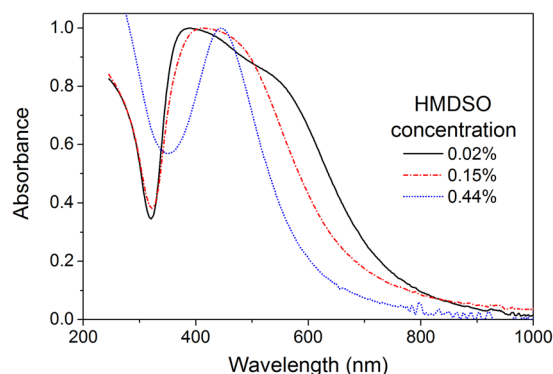


Figure 5. UV-Vis spectra of the core-shell nanoparticles prepared by GAS at different concentrations of HMDSO.

NPs. Adding oxygen to the Ar/HMDSO mixture permits tuning of the chemical composition of the shell from organosilicon plasma polymer to stoichiometric SiO_2 . The facile, single-step method presented here should lend itself to the controlled fabrication of other complex functional nanoparticles.

References

- Binns, C. Nanoclusters deposited on surfaces. *Surf. Sci. Rep.* **44**, 1–49 (2001).
- Cassidy, C. *et al.* Inoculation of silicon nanoparticles with silver atoms. *Sci. Rep.* **3**, 3083 (2013).
- Kortshagen, U. R. *et al.* Nonthermal Plasma Synthesis of Nanocrystals: Fundamental Principles, Materials, and Applications. *Chem. Rev.* **116**, 11061–11127 (2016).
- Wegner, K., Piseri, P., Tafreshi, H. V. & Milani, P. Cluster beam deposition: a tool for nanoscale science and technology. *J. Phys. D: Appl. Phys.* **39**, R439–R459 (2006).
- Solař, P. *et al.* Nylon-sputtered plasma polymer particles produced by a semi-hollow cathode gas aggregation source. *Vacuum* **111**, 124–130 (2015).
- Haberland, H., Karrais, M., Mall, M. & Thurner, Y. Thin films from energetic cluster impact: A feasibility study. *J. Vac. Sci. Technol. A* **10**, 3266–3271 (1992).
- Datta, D., Bhattacharyya, S. R., Shyjumon, I., Ghose, D. & Hippler, R. Production and deposition of energetic metal nanocluster ions of silver on Si substrates. *Surf. Coatings Technol.* **203**, 2452–2457 (2009).
- Kylián, O. *et al.* Deposition of Pt nanoclusters by means of gas aggregation cluster source. *Mater. Lett.* **79**, 229–231 (2012).
- Zhao, J. *et al.* Formation Mechanism of Fe Nanocubes by Magnetron Sputtering Inert Gas Condensation. *ACS Nano* **10**, 4684–4694 (2016).
- Belić, D., Chantry, R. L., Li, Z. Y. & Brown, S. A. Ag–Au nanoclusters: Structure and phase segregation. *Appl. Phys. Lett.* **99**, 171914 (2011).
- Velázquez-Palenzuela, A. *et al.* The enhanced activity of mass-selected Pt_xGd nanoparticles for oxygen electroreduction. *J. Catal.* **328**, 297–307 (2015).
- Chen, B., ten Brink, G. H., Palasantzas, G. & Kooi, B. J. Size-dependent and tunable crystallization of GeSbTe phase-change nanoparticles. *Sci. Rep.* **6**, 39546 (2016).
- Vernieres, J. *et al.* Gas Phase Synthesis of Multifunctional Fe-Based Nanocubes. *Adv. Funct. Mater.* 1605328, doi:10.1002/adfm.201605328 (2017).
- Xu, Y.-H. & Wang, J.-P. Direct Gas-Phase Synthesis of Heterostructured Nanoparticles through Phase Separation and Surface Segregation. *Adv. Mater.* **20**, 994–999 (2008).
- Tchaplyguine, M., Andersson, T., Zhang, C. & Björneholm, O. Core-shell structure disclosed in self-assembled Cu–Ag nanoalloy particles. *J. Chem. Phys.* **138**, 104303 (2013).
- Llamasa, D. *et al.* The ultimate step towards a tailored engineering of core@shell and core@shell@shell nanoparticles. *Nanoscale* **6**, 13483–13486 (2014).
- Caillard, A. *et al.* PdPt catalyst synthesized using a gas aggregation source and magnetron sputtering for fuel cell electrodes. *J. Phys. D: Appl. Phys.* **48**, 475302 (2015).
- Mayoral, A., Llamasa, D. & Huttel, Y. A novel Co@Au structure formed in bimetallic core@shell nanoparticles. *Chem. Commun.* **51**, 8442–8445 (2015).
- Elsukova, A. *et al.* Structure, morphology, and aging of Ag–Fe dumbbell nanoparticles. *Phys. status solidi* **208**, 2437–2442 (2011).
- Grammatikopoulos, P. *et al.* Kinetic trapping through coalescence and the formation of patterned Ag–Cu nanoparticles. *Nanoscale* **8**, 9780–9790 (2016).
- Li, X., Niitsoo, O. & Couzis, A. Electrostatically assisted fabrication of silver–dielectric core/shell nanoparticles thin film capacitor with uniform metal nanoparticle distribution and controlled spacing. *J. Colloid Interface Sci.* **465**, 333–341 (2016).
- Wang, Y. *et al.* Fabrication and high-performance microwave absorption of Ni@SnO₂@PPy Core-Shell composite. *Synth. Met.* **220**, 347–355 (2016).
- Zhou, W. *et al.* Dielectric properties and thermal conductivity of core-shell structured Ni@NiO/poly(vinylidene fluoride) composites. *J. Alloys Compd.* **693**, 1–8 (2017).
- Chaudhary, R. P., Mohanty, S. K. & Koymen, A. R. Novel method for synthesis of Fe core and C shell magnetic nanoparticles. *Carbon N. Y.* **79**, 67–73 (2014).
- Lei, P. & Girshick, S. L. PEGylation of gold-decorated silica nanoparticles in the aerosol phase. *Nanotechnology* **24**, 335602 (2013).
- Kylián, O., Choukurov, A. & Biederman, H. Nanostructured plasma polymers. *Thin Solid Films* **548**, 1–17 (2013).
- Biederman, H. *Plasma Polymer Films*. (Imperial College Press, 2004).
- Kuzminova, A. *et al.* From super-hydrophilic to super-hydrophobic surfaces using plasma polymerization combined with gas aggregation source of nanoparticles. *Vacuum* **110**, 58–61 (2014).
- Shelemin, a *et al.* Preparation of biomimetic nano-structured films with multi-scale roughness. *J. Phys. D: Appl. Phys.* **49**, 254001 (2016).
- Arkill, K. P., Mantell, J. M., Plant, S. R., Verkade, P. & Palmer, R. E. Using size-selected gold clusters on graphene oxide films to aid cryo-transmission electron tomography alignment. *Sci. Rep.* **5**, 9234 (2015).

31. Kratochvíl, J., Kuzminova, A., Kylián, O. & Biederman, H. Comparison of magnetron sputtering and gas aggregation nanoparticle source used for fabrication of silver nanoparticle films. *Surf. Coatings Technol.* **275**, 296–302 (2015).
32. Takele, H. *et al.* Tuning of electrical and structural properties of metal-polymer nanocomposite films prepared by co-evaporation technique. *Appl. Phys. A* **92**, 345–350 (2008).
33. Despax, B. & Raynaud, P. Deposition of ‘Polysiloxane’ Thin Films Containing Silver Particles by an RF Asymmetrical Discharge. *Plasma Process. Polym.* **4**, 127–134 (2007).
34. Saulou, C. *et al.* Plasma deposition of organosilicon polymer thin films with embedded nanosilver for prevention of microbial adhesion. *Appl. Surf. Sci.* **256**, S35–S39 (2009).
35. Peter, T. *et al.* Metal/polymer nanocomposite thin films prepared by plasma polymerization and high pressure magnetron sputtering. *Surf. Coatings Technol.* **205**, S38–S41 (2011).
36. Alissawi, N. *et al.* Plasma-polymerized HMDSO coatings to adjust the silver ion release properties of Ag/polymer nanocomposites. *J. Nanoparticle Res.* **15**, 2080 (2013).
37. Benelmekki, M. *et al.* A facile single-step synthesis of ternary multicore magneto-plasmonic nanoparticles. *Nanoscale* **6**, 3532 (2014).
38. Benelmekki, M. *et al.* On the formation of ternary metallic-dielectric multicore-shell nanoparticles by inert-gas condensation method. *Mater. Chem. Phys.* **151**, 275–281 (2015).
39. Kilicaslan, A. *et al.* Optical emission spectroscopy of microwave-plasmas at atmospheric pressure applied to the growth of organosilicon and organotitanium nanopowders. *J. Appl. Phys.* **115**, 113301 (2014).
40. Maicu, M. *et al.* Synthesis and deposition of metal nanoparticles by gas condensation process. *J. Vac. Sci. Technol. A Vacuum, Surfaces, Film.* **32**, 02B113 (2014).

Acknowledgements

This work was supported by the grant GACR 13–09853 S from the Grant Agency of the Czech Republic. It was also supported by the German Research Foundation (DFG) within the framework of the Collaborative Research Center SFB Transregio 24, subproject B13.

Author Contributions

Pavel Solař conceived and conducted the experiments and analyzed the results, Oleksandr Polonskyi conceived the experiment and analyzed the results, Ansgar Olbricht conducted the experiments, Alexander Hinz measured the TEM, Artem Shelemin measured the FTIR, Ondřej Kylián revised the manuscript, Andrei Choukourou analyzed the data and revised the manuscript, Franz Faupel is the project leader in Kiel University and coordinated the work on Germany side, Hynek Biederman is the project leader in Charles University and coordinated the work on the side of Czech Republic.

Additional Information

Competing Interests: The authors declare that they have no competing interests.

Publisher's note: Springer Nature remains neutral with regard to jurisdictional claims in published maps and institutional affiliations.



Open Access This article is licensed under a Creative Commons Attribution 4.0 International License, which permits use, sharing, adaptation, distribution and reproduction in any medium or format, as long as you give appropriate credit to the original author(s) and the source, provide a link to the Creative Commons license, and indicate if changes were made. The images or other third party material in this article are included in the article's Creative Commons license, unless indicated otherwise in a credit line to the material. If material is not included in the article's Creative Commons license and your intended use is not permitted by statutory regulation or exceeds the permitted use, you will need to obtain permission directly from the copyright holder. To view a copy of this license, visit <http://creativecommons.org/licenses/by/4.0/>.

© The Author(s) 2017